

**8.10 NONLINEAR INTERACTION BETWEEN THE DIURNAL AND SEMIDIURNAL TIDES: TERDIURNAL AND DIURNAL SECONDARY WAVES**

H. Teitelbaum and F. Vial

Laboratoire de Meteorologie Dynamique du CNRS  
Ecole Polytechnique, 91128 Palaiseau Cedex, France

A. H. Manson

Institute of Space and Atmospheric Studies  
University of Saskatchewan, Saskatoon, Saskatchewan, Canada S7N OWO

R. Giraldez

Laboratorio Ionosferico de la Armada de la Republica Argentina  
SENID and CONICET, Av. del Libertador 327, 1839 Vicente Lopez  
Province Buenos Aires, Republica Argentina

M. Masseboeuf

CNET, CNRS, CRPE  
4 Avenue de Neptune  
94107 Saint-Maur des Fosses, France

Many years of measurements obtained using French meteor radars at Garchy (latitude 47°N) and Montpazier (latitude 44°N) are used to show the existence of an 8-hour oscillation. Some examples of the structure of this wave are displayed and compared with measurements performed at Saskatoon (latitude 52°N) and Budrio (latitude 45°N). This wave can be interpreted as the solar-driven terdiurnal tide, or as the result of the nonlinear interaction between the diurnal and semidiurnal tides. Both hypotheses are tested with numerical models. Incidentally, the possible existence of a 24-hour wave resulting from this interaction is also studied.

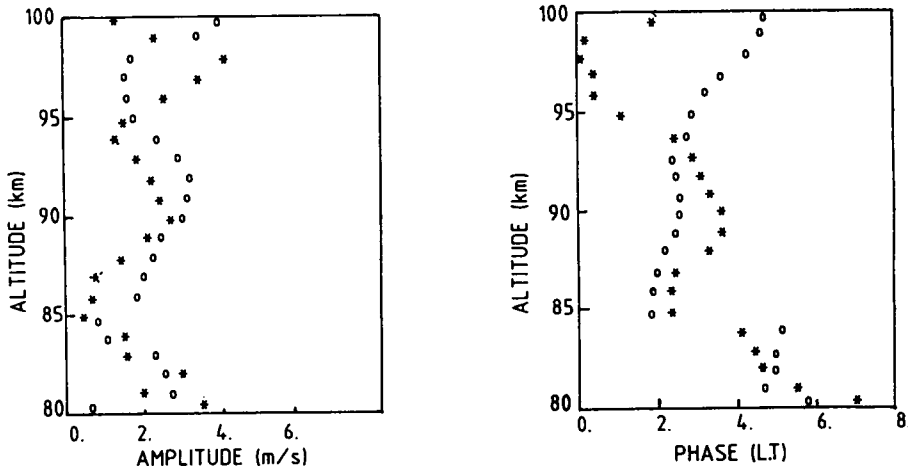


Figure 1. Amplitude and phase of terdiurnal tide (eastward wind), deduced from two simultaneous campaigns carried out at Garchy (47°N) and Montpazier (44°N) during the 8-20 July 1976 period.  
o - Garchy, \* - Montpazier.

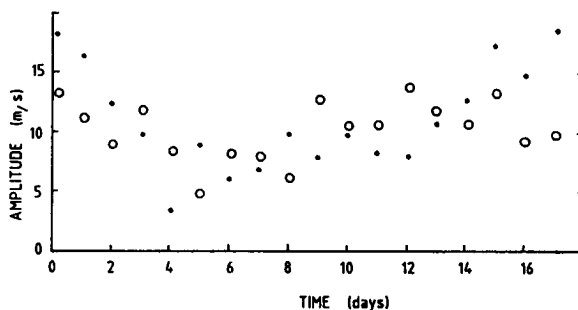


Figure 2. Short-time variation of the diurnal and terdiurnal tides for a single campaign. Garchy, 6 to 28 January 1976 period. Mean  $<90 - 95\text{ km}>$  eastward wind • - diurnal tide, ○ - terdiurnal tide.

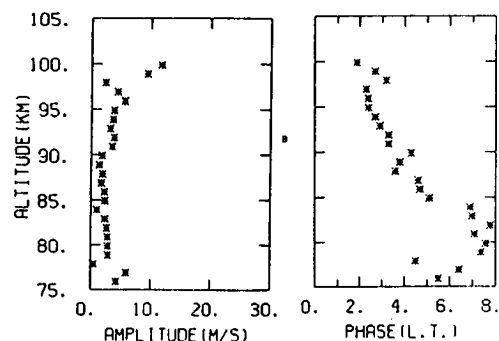
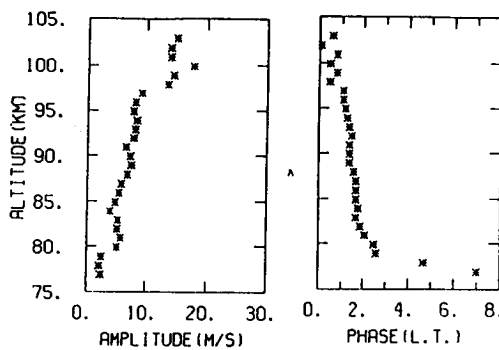


Figure 3. Terdiurnal monthly mean climatology for typical winter (a) and summer (b) months. Eastward wind at Garchy ( $47^\circ\text{N}$ ).

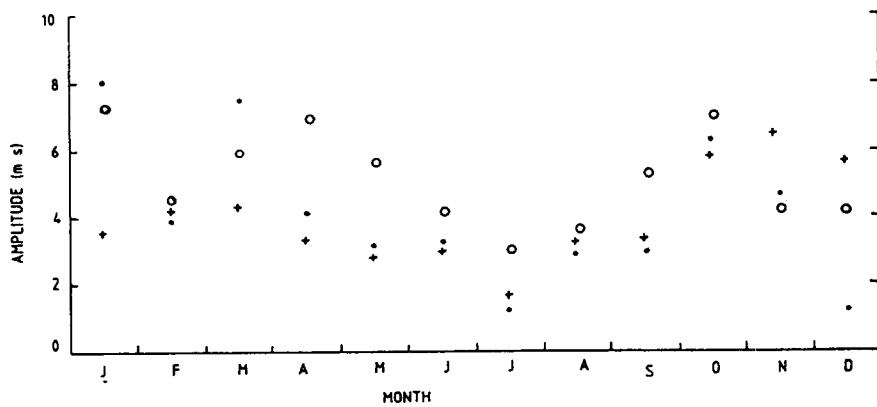


Figure 4a. Terdiurnal monthly mean climatology for all the months of the year and 94 km altitude: amplitude of the eastward wind at three different latitudes. • - Garchy ( $47^{\circ}\text{N}$ ), + - Montpazier ( $44^{\circ}\text{N}$ ), o - Saskatoon ( $52^{\circ}\text{N}$ ).

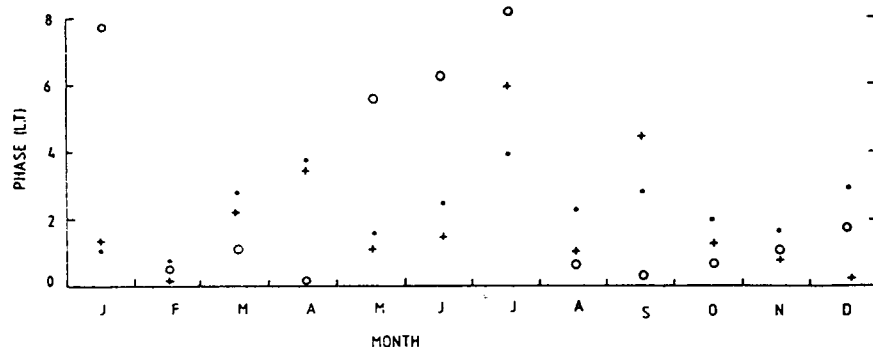


Figure 4b. The same as Figure 4a but for the phase. • - Garchy ( $47^{\circ}\text{N}$ ), + - Montpazier ( $44^{\circ}\text{N}$ ), o - Saskatoon ( $52^{\circ}\text{N}$ ).

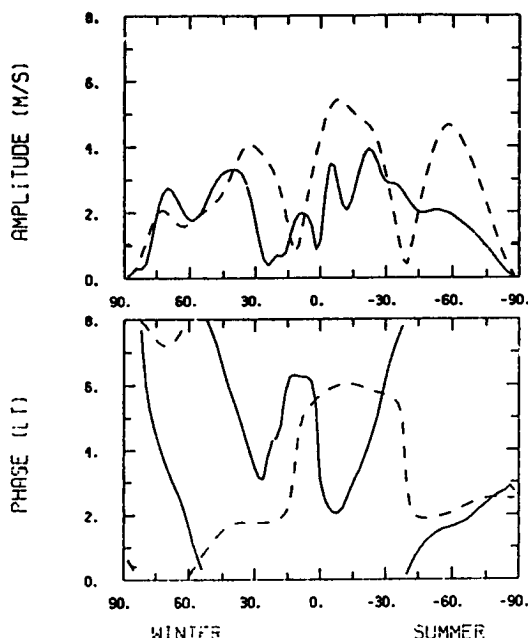


Figure 5. Latitudinal variation of the terdiurnal tide (eastward wind), for solstice conditions at 95 km altitude. The theoretical solar-driven and nonlinear waves are shown. The nonlinear wave is a secondary wave generated by the nonlinear interaction of the diurnal and semidiurnal tides. - - - solar-driven wave, — - nonlinear wave.

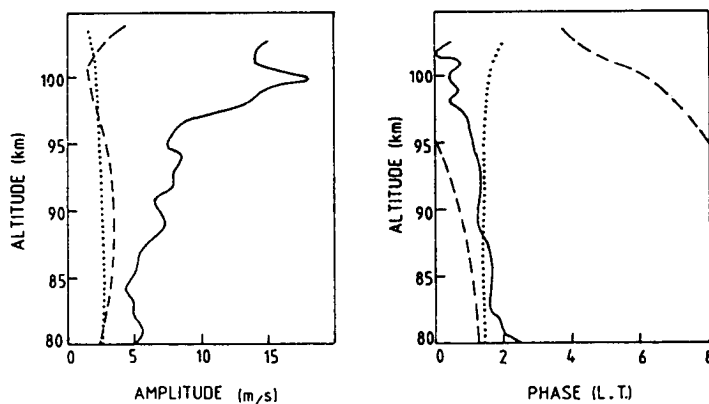


Figure 6. Eastward wind profile corresponding to the terdiurnal tide at  $47^{\circ}$  latitude in winter. Comparison of the data with the calculated solar-driven wave and with the superposition of the solar-driven and the nonlinear waves. — - data, . . . . - solar-driven, - - - - solar-driven plus nonlinear.

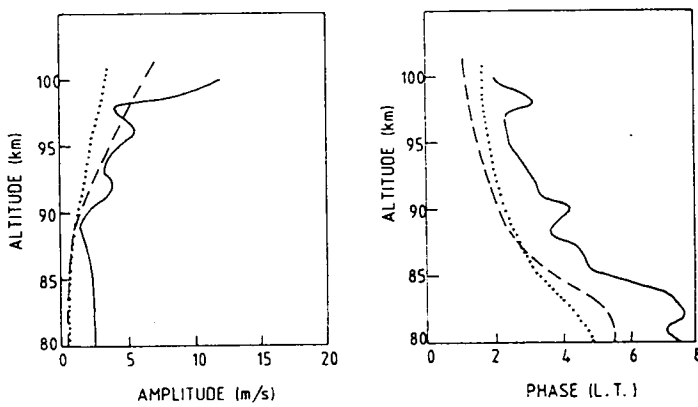


Figure 7. The same as in Figure 6 but in summer.

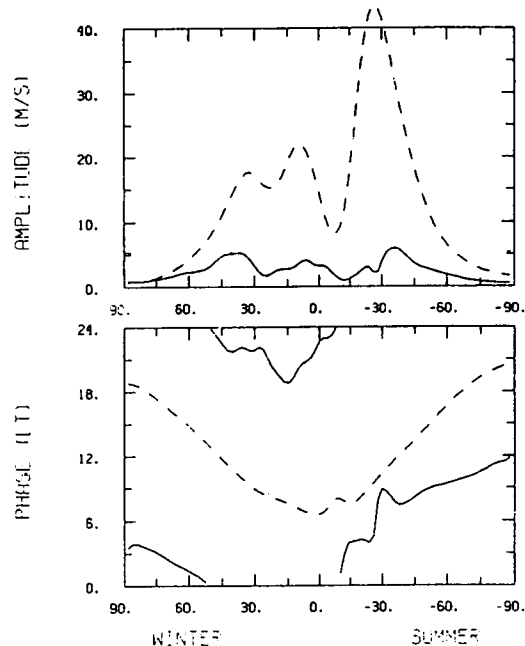


Figure 8. Latitudinal variation of the amplitude and phase of the diurnal nonlinear secondary wave for solstice conditions at 95 km altitude. The solar-driven diurnal tide is also shown. — nonlinear secondary diurnal tide, - - - solar-driven diurnal tide.